Supporting Information

In situ metallization of 2D COFs with acid/base sites synergistic effects for boosting one-pot CO_2 conversion

Yi Yu,[a] Meng Wang,[a] Ying Wu *[bc] and Hongxia Xi *[a]

[a] School of Chemistry and Chemical Engineering, South China University of Technology, Guangzhou 510640, China.

[b] School of Chemical Engineering and Light Industry, Guangdong University of Technology, Guangzhou 510006, P. R. China.

[c] Jieyang Branch of Chemistry and Chemical Engineering Guangdong Laboratory (Rongjiang Laboratory), Jieyang 515200, P. R. China.

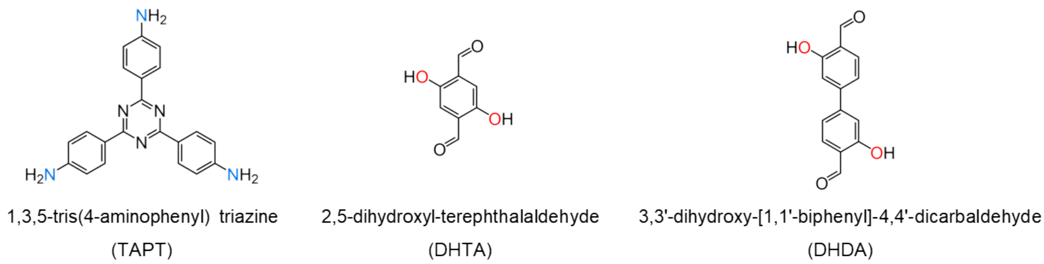

Fig. S1. Molecule structures of linkers.

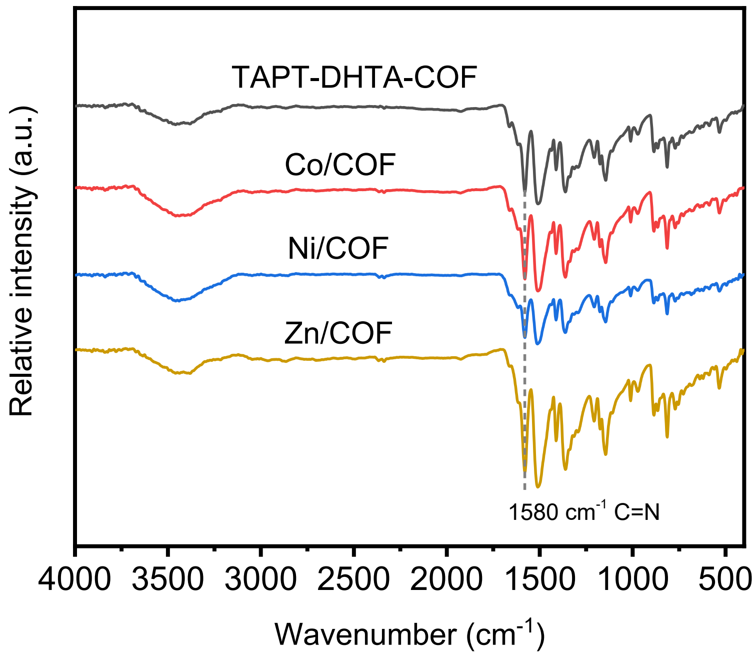

Fig. S2. FTIR spectrum of COF materials.

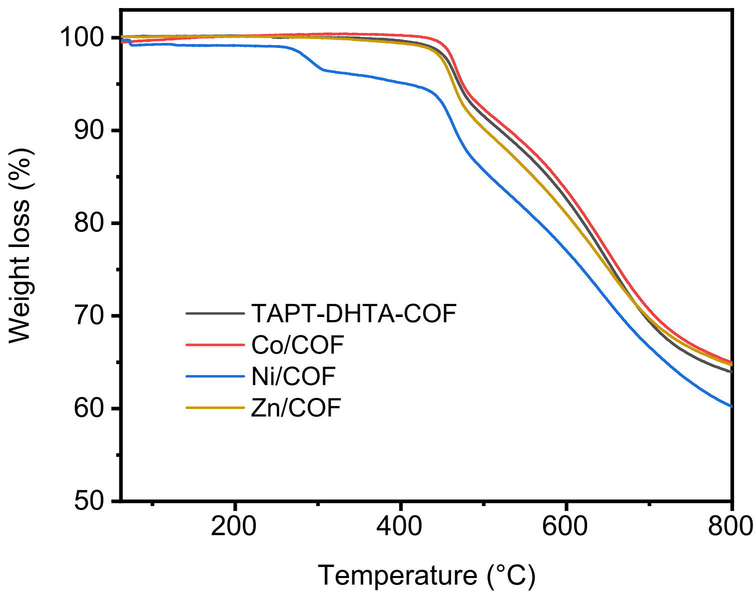

Fig. S3. TGA curves of COF materials.

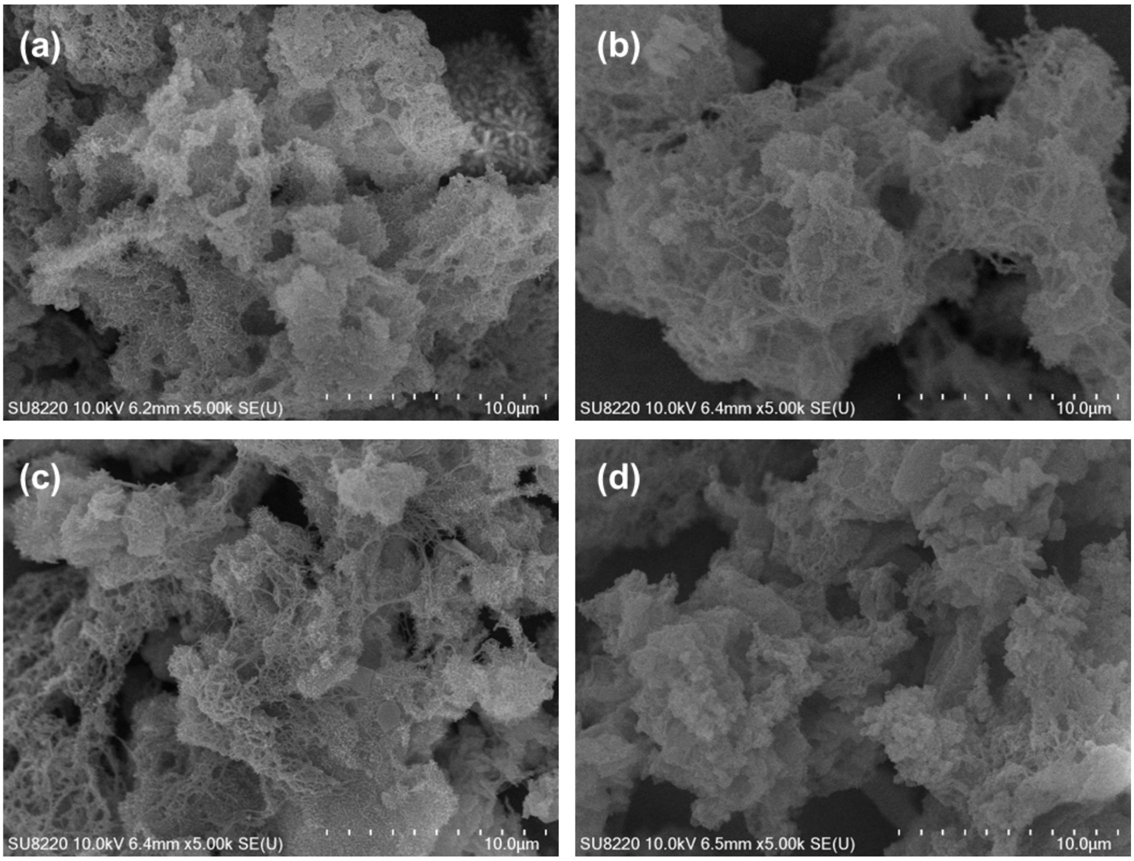

Fig. S4. SEM images of (a) TAPT-DHTA-COF, (b) Co/COF, (c) Ni/COF and (d) Zn/COF.

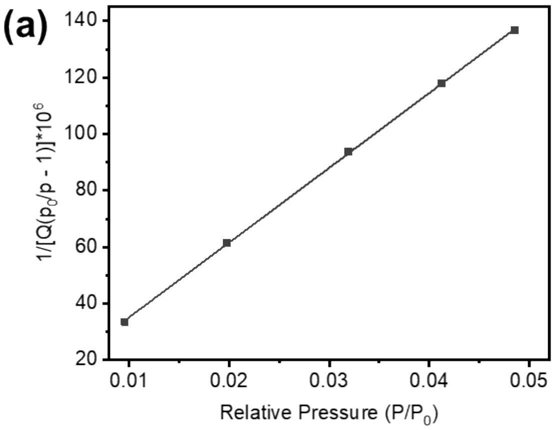

(b)

P/P_0 Range	0.008-0.050
Correlation Coefficient	0.9999
C	303.1
Q_m	337.0101 cm^3/g STP
BET Surface Area	1641 m^2/g

Fig. S5. BET analysis of TAPT-DHTA-COF.

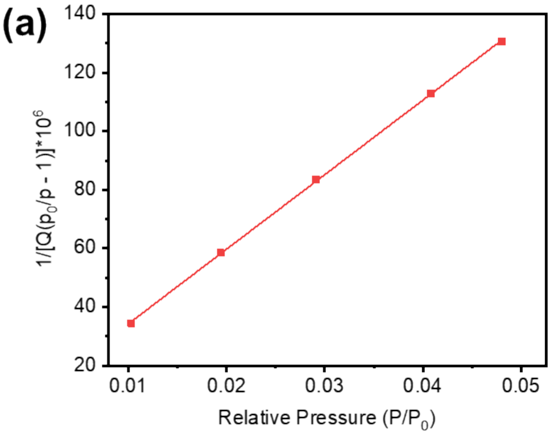

(b)

P/P_0 Range	0.01-0.050
Correlation Coefficient	0.9999
C	292.6
Q_m	390.8928 cm^3/g STP
BET Surface Area	1701 m^2/g

Fig. S6. BET analysis of Co/COF.

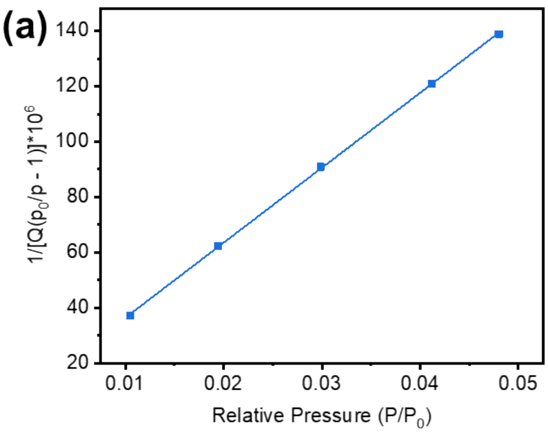

(b)

P/P_0 Range	0.01-0.050
Correlation Coefficient	0.9999
C	292.5
Q_m	367.8048 cm^3/g STP
BET Surface Area	1601 m^2/g

Fig. S7. BET analysis of Ni/COF.

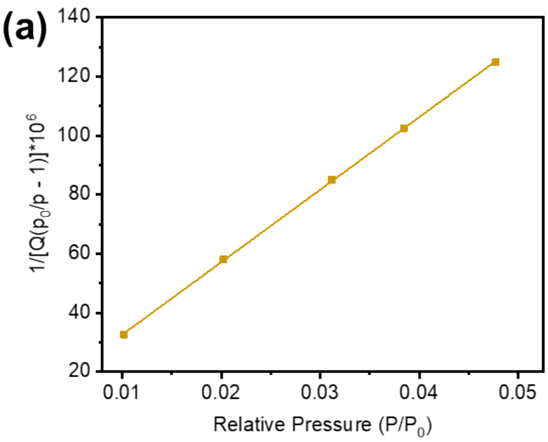

(b)

P/P_0 Range	0.009-0.050
Correlation Coefficient	0.9999
C	306.5
Q_m	406.0644 cm^3/g STP
BET Surface Area	1767 m^2/g

Fig. S8. BET analysis of Zn/COF.

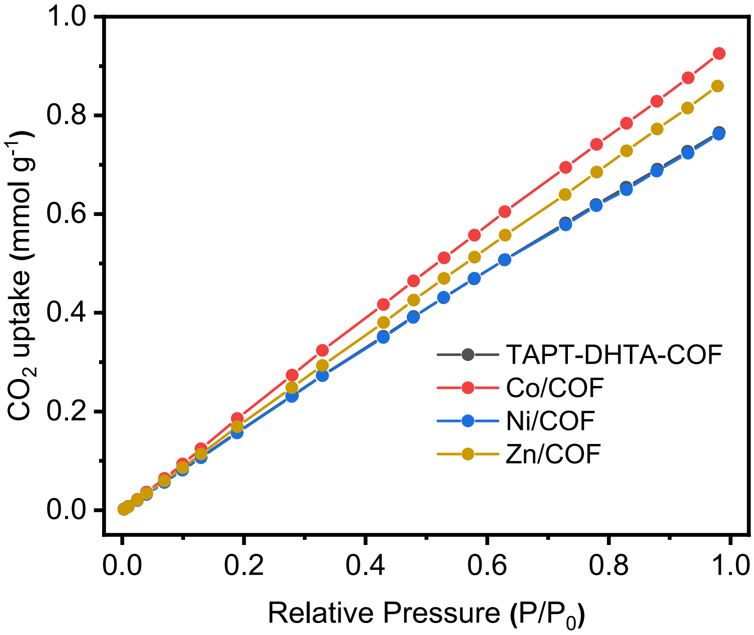

Fig. S9. CO_2 adsorption curves of TAPT-DHTA-COF series at 298 K.

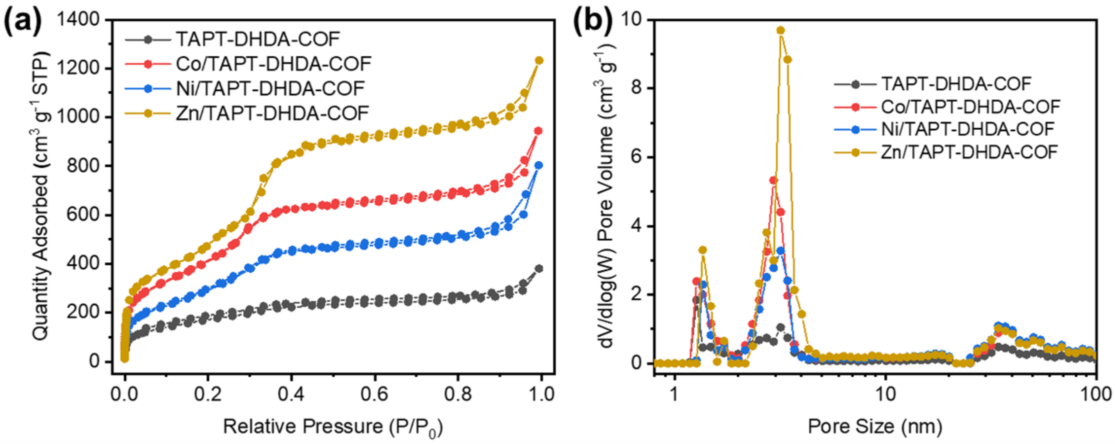

Fig. S10. (a) N_2 sorption isotherms and (c) pore distribution of TAPT-DHDA-COF series.

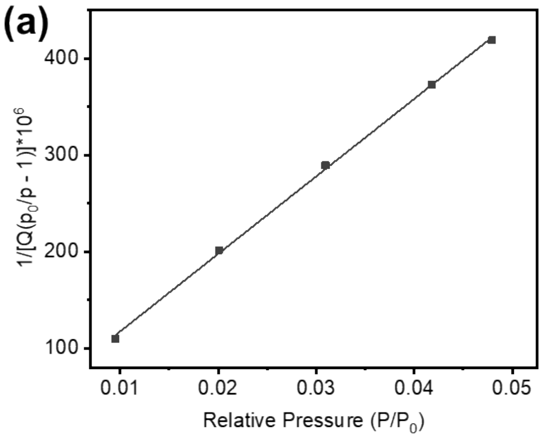

(b)

P/P_0 Range	0.006-0.050
Correlation Coefficient	0.9996
C	218.2
Q_m	123.9571 cm^3/g STP
BET Surface Area	540 m^2/g

Fig. S11. BET analysis of TAPT-DHDA-COF.

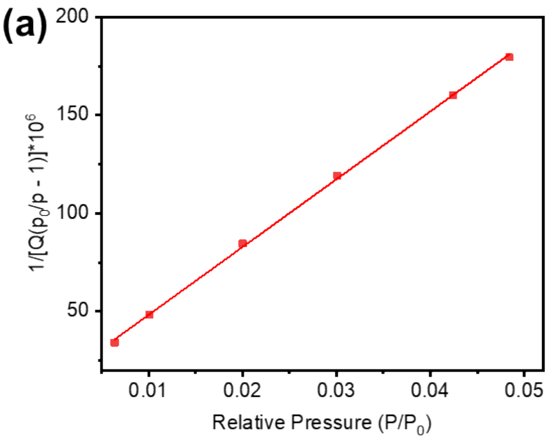

(b)

P/P_0 Range	0.006-0.063
Correlation Coefficient	0.9997
C	254.7
Q_m	287.8155 cm^3/g STP
BET Surface Area	1253 m^2/g

Fig. S12. BET analysis of Co/TAPT-DHDA-COF.

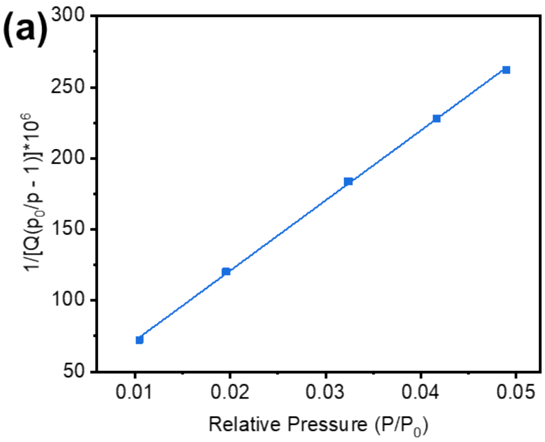

(b)

P/P_0 Range	0.007-0.064
Correlation Coefficient	0.9998
C	217.8
Q_m	202.2368 cm^3/g STP
BET Surface Area	880 m^2/g

Fig. S13. BET analysis of Ni/TAPT-DHDA-COF.

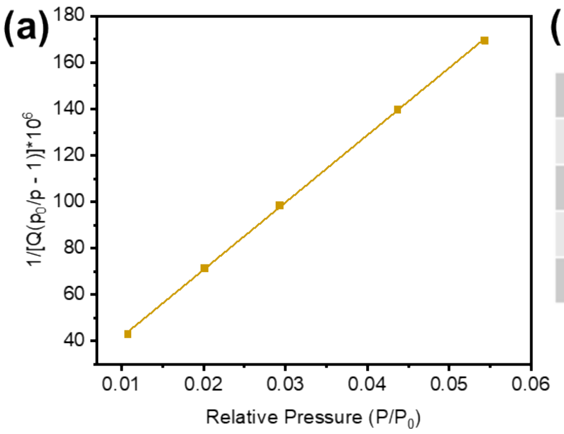

(b)

P/P_0 Range	0.007-0.064
Correlation Coefficient	0.9999
C	225.3
Q_m	343.7196 cm^3/g STP
BET Surface Area	1496 m^2/g

Fig. S14. BET analysis of Zn/TAPT-DHDA-COF.

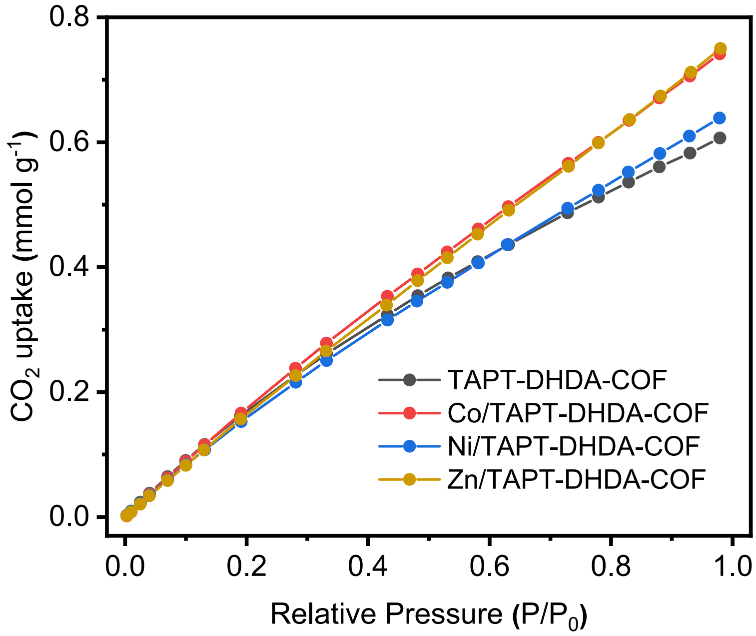

Fig. S15. CO_2 adsorption curves of TAPT-DHDA-COF series at 298 K.

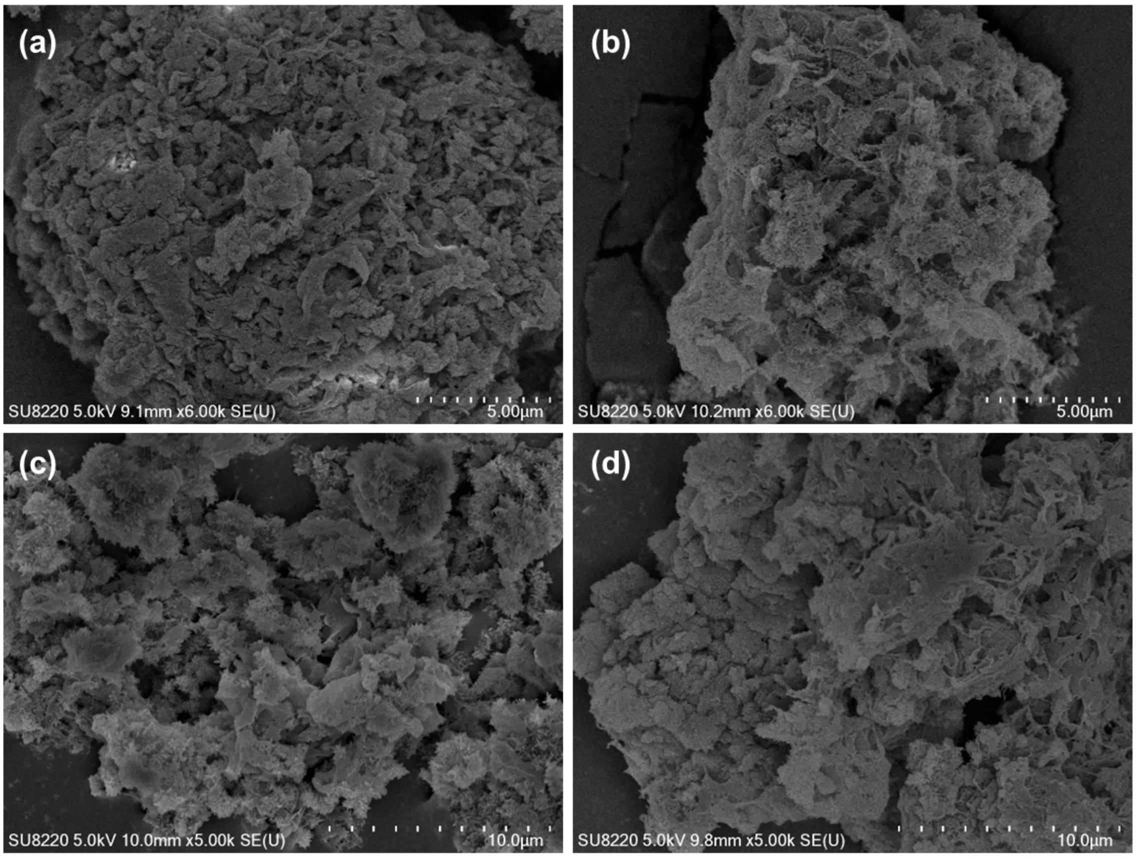

Fig. S16. SEM images of (a) TAPT-DHDA-COF, (b) Co/TAPT-DHDA-COF, (c) Ni/TAPT-DHDA-COF and (d) Zn/TAPT-DHDA-COF.

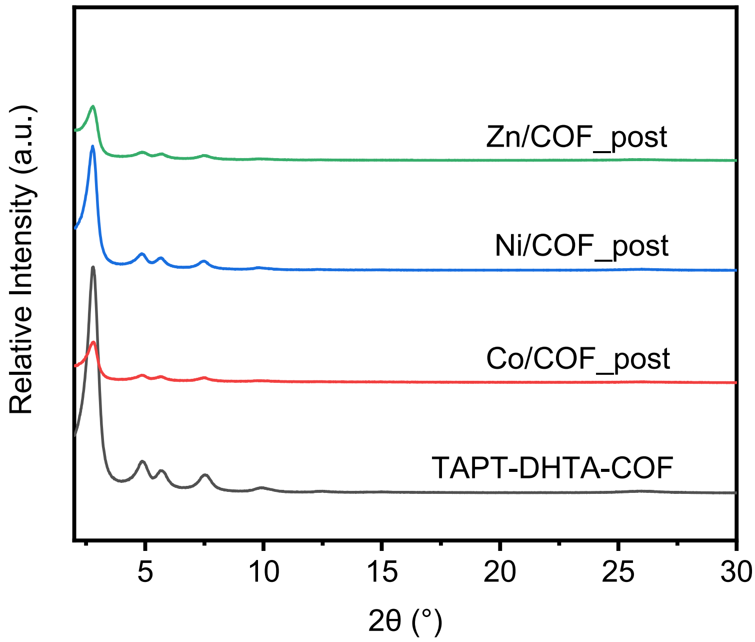

Fig. S17. XRD patterns of M/COF_post materials.

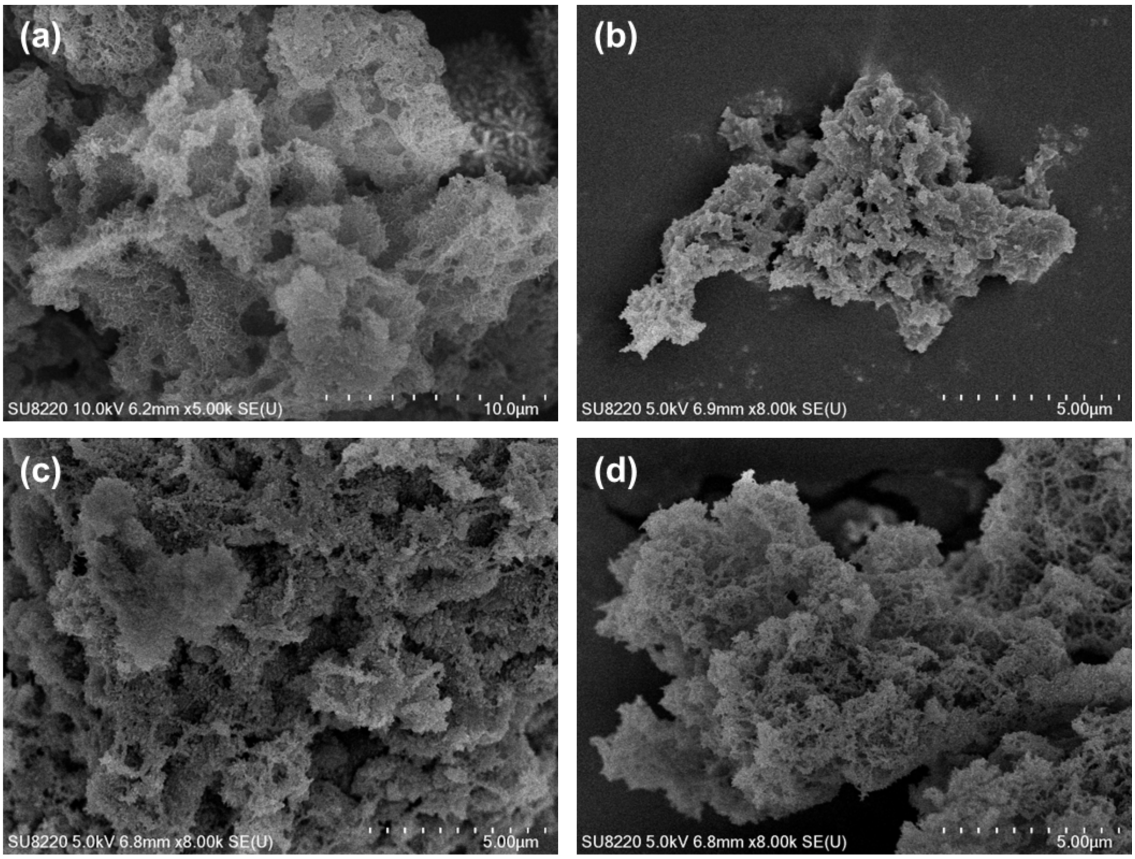

Fig. S18. SEM images of (a) TAPT-DHTA-COF, (b) Co/COF_post, (c) Ni/COF_post and (d) Zn/COF_post.

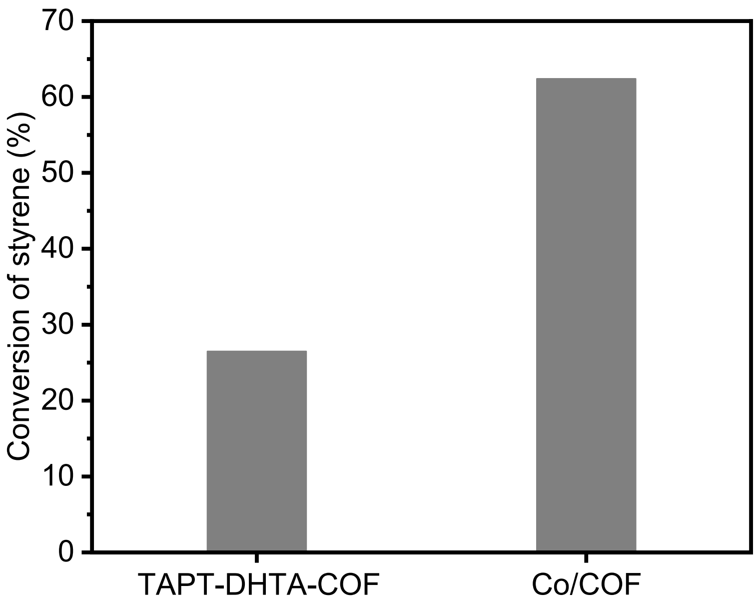

Fig. S19. Conversion of styrene towards styrene epoxidation reaction. Reaction conditions: styrene (2 mmol), catalysts (10 mg), TBHP in decane (1 mL), N_2 (balloon pressure, 1 bar), 80 ºC, 4 h.

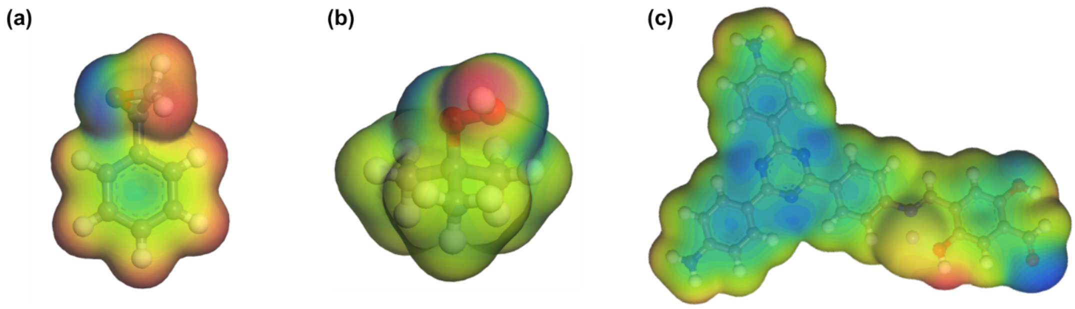

Fig. S20. Electrostatic potential distributions of (a) styrene oxide, (b) TBHP and (c) Co/COF.

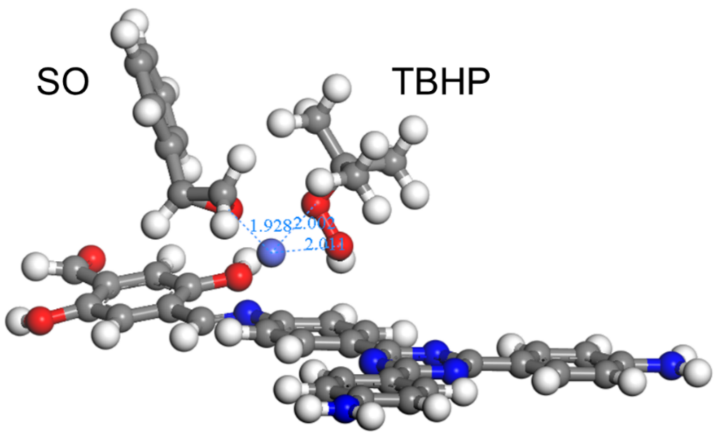

Fig. S21. The calculated distance between SO/TBHP and Co/COF.

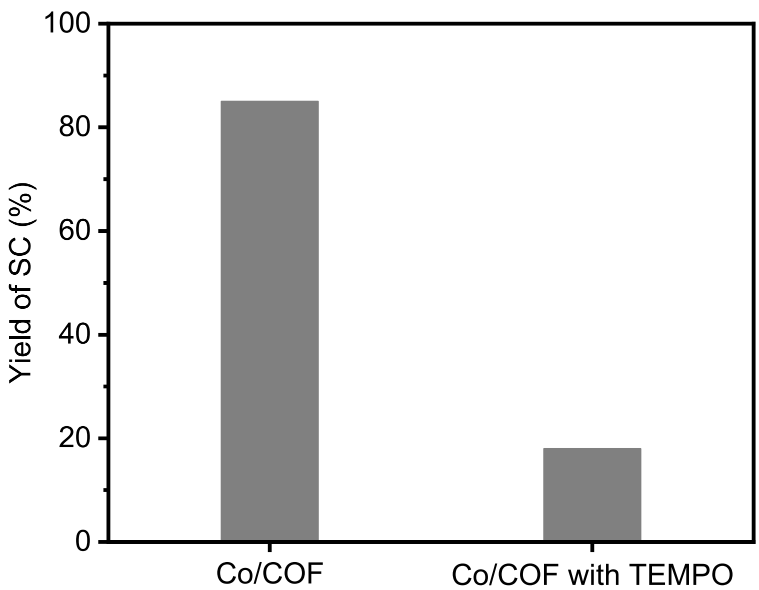

Fig. S22. Change in catalytic performances of COF/Co with 2,2,6,6-Tetramethylpiperidine 1oxyl (TEMPO).

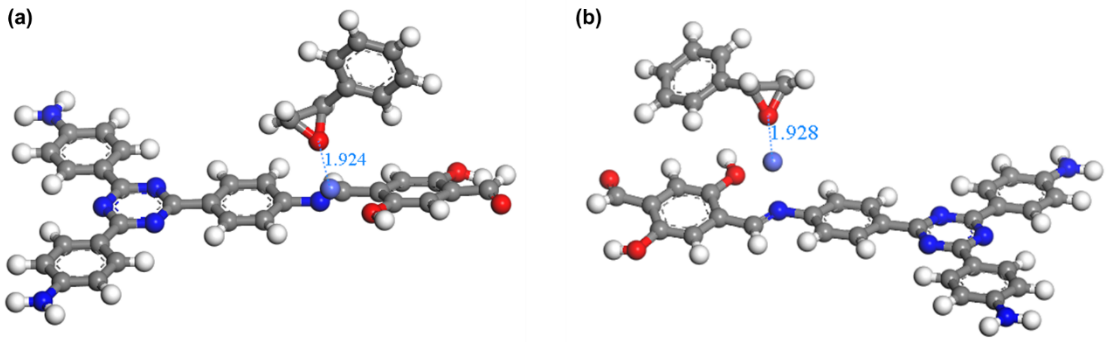

Fig. S23. The optimal results of the interaction of SO with (a) Co sites and (b) -OH sites.

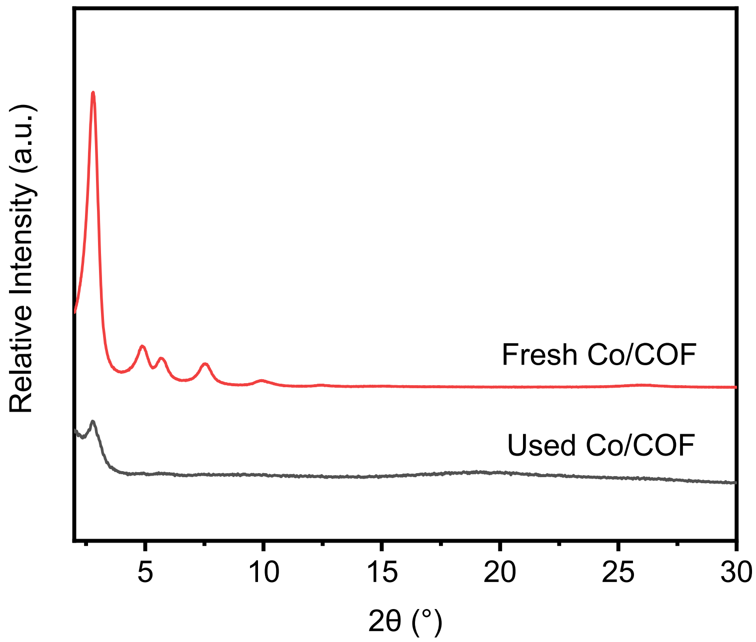

Fig. S24. XRD pattern of Co/COF after being used.

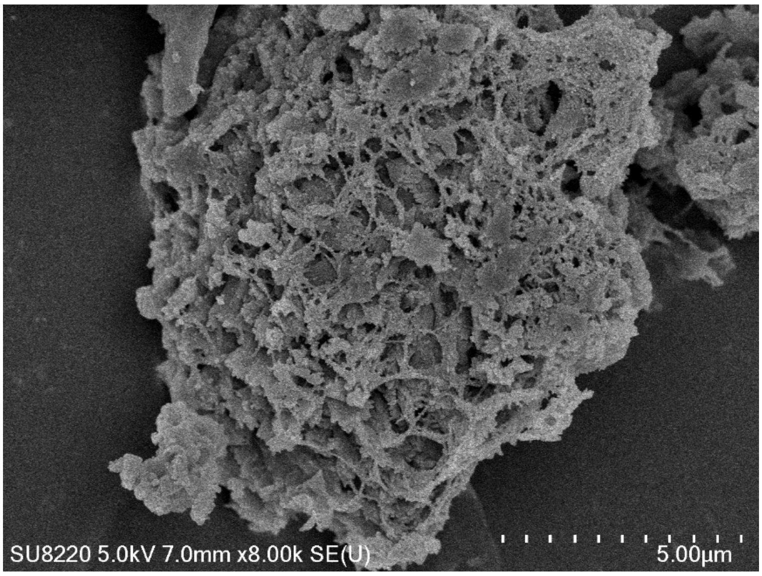

Fig. S25. SEM image of Co/COF after being used.

Table S1. Physicochemical properties of TAPT-DHTA-COF series.

Sample	Metal content (wt%)	S_{BET} (m^2 g^{-1})	V_t (cm^3 g^{-1})	CO_2 uptake at 298 K (mmol g^{-1})
TAPT-DHTA-COF	-	1641	1.66	0.76
Co/COF	0.56	1701	1.71	0.93
Ni/COF	2.55	1601	1.58	0.77
Zn/COF	0.60	1767	1.68	0.86

Table S2. Physicochemical properties of TAPT-DHDA-COF series.

Sample	S_{BET} (m^2 g^{-1})	V_t (cm^3 g^{-1})	CO_2 uptake at 298 K (mmol g^{-1})
TAPT-DHDA-COF	540	0.57	0.61
Co/TAPT-DHDA-COF	1253	1.43	0.74
Ni/TAPT-DHDA-COF	880	1.20	0.64
Zn/TAPT-DHDA-COF	1496	1.86	0.75

Table S3. COFs catalyzed one-pot reaction of styrene and CO_2.[a]

Entry	Catalyst	Conversion of styrene (%)	Yield of SC (%)
1	TAPT-DHDA-COF	87	53
2	Co/TAPT-DHDA-COF	95	84
3	Ni/TAPT-DHDA-COF	87	70
4	Zn/TAPT-DHDA-COF	90	75

[a] Reaction conditions: styrene (2 mmol), catalysts (10 mg), TBHP in decane (1 mL), CO_2 (balloon pressure, 1 bar), 80 ºC, 24 h.

Table S4. COFs catalyzed one-pot reaction of styrene and CO_2.[a]

Entry	Catalyst	Conversion of styrene (%)	Yield of SC (%)

1	TAPT-DHTA-COF	87	56
2	Co/COF_post	97	71
3	Ni/COF_post	84	55
4	Zn/COF_post	86	55

[a] Reaction conditions: styrene (2 mmol), catalysts (10 mg), TBHP in decane (1 mL), CO_2 (balloon pressure, 1 bar), 80 ºC, 24 h.

Table S5. Comparison of Co/COF against other reported heterogeneous catalysts for the one-pot tandem catalysis.

Catalyst + co-catalyst	T (°C)	P (bar)	t (h)	Conv. of sty. (%)	Yield of SC (%)	Ref.
CeO_2 + TBAB	80	20	24	97	90	[1]
Titanium-silicate + TBAB	70	8	48	92	64	[2]
$Co(acac)_2$-QPB@MCS	100	35	48	95	66	[3]
ADD-FeAl + TBAB	70	5	8	97	88	[4]
$N(CH_3)_2$-[Im][HCO_3]@SBA-15	80	10	28	95	82	[5]
ImBr-MOF-545(Mn)	60	5	10	99	94	[6]
ZnW PYI1 + TBAB	50	5	96	92	73	[7]
CSMCRI-10 + TBAB	80	8	8	93	88	[8]
Co(II)@CSUST-2 + TBAB	75	1	12	98	84	[9]
Cr-MIL-101 + TBAB	24	8	24	39	7	[10]
MOF-590 + TBAB	80	1	10	93	87	[11]
Fe^{III}@MOF1 + TBAB	50	8	24	99	64	[12]
NiBDC NS + TBAB	80	1	12	95	87	[13]
CoBDC	100	1	12	92	85	[14]
Zr-BTB/PA-Co	80	1	12	94	93	[15]
Co/COF	80	1	24	99	85	This work

References

1 S. Zhang, Z. Xia, Y. Zou, F. Cao, Y. Liu, Y. Ma and Y. Qu, *J. Am. Chem. Soc.*, 2019, **141**, 11353-

11357.
2 N. V. Maksimchuk, I. D. Ivanchikova, A. B. Ayupov and O. A. Kholdeeva, *Appl. Catal. B-Environ.*, 2016, **181**, 363-370.
3 S. Kumar, N. Singhal, R. K. Singh, P. Gupta, R. Singh and S. L. Jain, *Dalton T.*, 2015, **44**, 11860-11866.
4 Q. Yang, Z. Lu, L. Chen, Y. Wang, Z. Tian, K. Tong, X. Tang, N. Zhang, J. Zhou, L. Zhang, Q. Zhang, S. Dai and Y. Lin, *Nano Lett.*, 2022, **22**, 8381-8388.
5 Z. Tianxiang, L. Guangcai, L. Hua, X. Wenjie and H. Xingbang, *Micropor. Mesopor. Mater.*, 2023, **293**, 109779.
6 K. Yu, P. Puthiaraj and W.-S. Ahn, *Appl. Catal. B-Environ.*, 2020, **273**, 119059.
7 Q. Han, B. Qi, W. Ren, C. He, J. Niu and C. Duan, *Nat. Commun.*, 2015, **6**, 10007.
8 N. Seal, K. Karthick, M. Singh, S. Kundu and S. Neogi, *Chem. Eng. J.*, 2022, **429**, 132301.
9 H.-G. Jin, F. Chen, H. Zhang, W. Xu, Y. Wang, J. Fan and Z.-S. Chao, *J. Mater. Sci.*, 2020, **55**, 16184-16196.
10 O. V. Zalomaeva, N. V. Maksimchuk, A. M. Chibiryaev, K. A. Kovalenko, V. P. Fedin and B. S. Balzhinimaev, *J. Energy Chem.*, 2013, **22**, 130-135.
11 H. T. D. Nguyen, Y. B. N. Tran, H. N. Nguyen, T. C. Nguyen, F. Gandara and P. T. K. Nguyen, *Inorg. Chem.*, 2018, **57**, 13772-13782.
12 N. Sharma, S. S. Dhankhar, S. Kumar, T. J. D. Kumar and C. M. Nagaraja, *Chem.-A Eur. J.*, 2018, **24**, 16662-16669.
13 Y. Yu, X. Chen, X. Wang, X. Feng, S. Liu, C. Duan, Y. Wu and H. Xi, *Chem. Eng. Sci.*, 2023, **278**, 118898.
14 X. Chen, S. Liu, C. Duan, Y. Yu and H. Xi, *Ind. Eng. Chem. Res.*, 2024, **63**, 5629-5636.
15 Y. Yu, X. Feng, Z. Xie, Y. Wu and H. Xi, *AIChE J.* 2023, **70**, e18290.